Am J Physiol Renal Physiol 299: F1178–F1184, 2010.
First published August 11, 2010; doi:10.1152/ajprenal.00152.2010.

Nucleofection disrupts tight junction fence function to alter membrane polarity of renal epithelial cells

Di Mo,[1] Beth A. Potter,[1] Carol A. Bertrand,[2] Jeffrey D. Hildebrand,[3] Jennifer R. Bruns,[1] and Ora A. Weisz[1,2]

[1]*Renal Electrolyte Division and* [2]*Department of Cell Biology and Physiology, University of Pittsburgh School of Medicine, and* [3]*Department of Biological Sciences, University of Pittsburgh, Pittsburgh, Pennsylvania*

Submitted 10 March 2010; accepted in final form 6 August 2010

Mo D, Potter BA, Bertrand CA, Hildebrand JD, Bruns JR, Weisz OA. Nucleofection disrupts tight junction fence function to alter membrane polarity of renal epithelial cells. *Am J Physiol Renal Physiol* 299: F1178–F1184, 2010. First published August 11, 2010; doi:10.1152/ajprenal.00152.2010.—Here, we compared the effects of nucleofection and lipid-based approaches to introduce siRNA duplexes on the subsequent development of membrane polarity in kidney cells. Nucleofection of Madin-Darby canine kidney (MDCK) cells, even with control siRNA duplexes, disrupted the initial surface polarity as well as the steady-state distribution of membrane proteins. Transfection using lipofectamine yielded slightly less efficient knockdown but did not disrupt membrane polarity. Polarized secretion was unaffected by nucleofection, suggesting a selective defect in the development of membrane polarity. Cilia frequency and length were not altered by nucleofection. However, the basolateral appearance of a fluorescent lipid tracer added to the apical surface of nucleofected cells was dramatically enhanced relative to untransfected controls or lipofectamine-treated cells. In contrast, [^{3}H]inulin diffusion and transepithelial electrical resistance were not altered in nucleofected cells compared with untransfected ones. We conclude that nucleofection selectively hinders development of the tight junction fence function in MDCK cells.

transfection; siRNA; MDCK; apical; basolateral; galectin-3

THE DEVELOPMENT OF METHODS to introduce heterologous DNA and RNA into cultured cells by transient transfection has revolutionized the study of protein function. Moreover, the recent introduction of RNA silencing technologies has provided a powerful tool to manipulate the spectrum of cellular functions and a potential therapeutic strategy for various diseases. Calcium-phosphate-, cationic lipid-, viral-, and electroporation-based approaches are among the most common methods for this purpose. Inherent in these approaches is the requirement that cell function or morphology is not significantly affected by the experimental manipulation itself. However, the mechanisms by which these approaches enable DNA/RNA passage into cells remain largely obscure.

Polarized cells represent a unique challenge to transfection. The plasma membrane of these cells is delineated by tight junctions (TJs) into two asymmetric compartments: an apical domain and a basolateral domain. The polarized delivery of receptors and ion transporters to these domains is critical for proper function of these cells. Traditionally, polarized epithelial cells have been recalcitrant to transient transfection. Transfection of these cells before polarization generally enhances efficiency; however, expression of the heterologous DNA/RNA may be significantly reduced by the time the cells attain a fully differentiated phenotype. A relatively new approach that has proven useful is nucleofection of DNA and RNA into cells in suspension. Delivery of foreign nucleic acid substrates directly into the nucleus apparently enhances the efficiency of transfection without compromising cellular viability (9, 10). This method has been successfully adapted to transfect polarized renal cells and is becoming increasingly popular (4).

In optimizing approaches to transfect cells with siRNA duplexes, we observed that nucleofection of cells, even with control siRNAs, resulted in an unexpected but reproducible decrease in cell polarity of apical membrane proteins in Madin-Darby canine kidney (MDCK) and other renal eptihelial cells, even when cultured for up to 5 days on permeable supports after the procedure. Nevertheless, polarized secretion of heterologously expressed and endogenous proteins was unaffected by this maneuver. The decrease in membrane polarity was not due to the absence of TJs as ZO-1 staining patterns were similar in control vs. nucleofected cells. Moreover, cilia length and frequency were indistinguishable in nucleofected vs. control cells. The gate function of TJs was also intact as measured by transepithelial resistance (TER) and paracellular transport of inulin. However, diffusion of an apically added fluorescent lipid probe to the basolateral surface was dramatically enhanced in cells that had been nucleofected before plating. We conclude that nucleofection disrupts the development and function of TJs in MDCK cells that precludes use of this approach to examine polarized trafficking.

MATERIALS AND METHODS

Cell culture, virus production, and adenoviral infection. MDCK II cells were grown in DMEM (Sigma) with 10% FBS and 1% penicillin/streptomycin. Murine cortical collecting duct (CCD) mpkCCD$_{c14}$ cells were cultured as previously described (2). Replication-defective recombinant adenovirus encoding YFP-p75 was originally provided by E. Rodriguez-Boulan. Tetracycline-transactivator-inducible adenoviruses encoding rat endolyn, truncated endolyn (ensol), and influenza hemagglutinin (HA) were generated using the Cre-Lox system or were described previously (11, 12). MDCK cells stably expressing the tetracycline transactivator were infected with recombinant adenoviruses as described in and used for experiments the following day (13).

Nucleofection of siRNA duplexes. MDCK cells in suspension (4×10^6/cuvette) were nucleofected with 10 μg siRNA duplexes using program T23 according to Amaxa Nucleofector instructions in 100 μl Ingenio electroporation solution (Mirus). SiRNA duplexes were purchased from Dharmacon. Unless noted otherwise, cells were then incubated overnight in tissue culture dishes in RPMI medium supplemented with 10% FBS, and then trypsinized, counted, and plated (0.5×10^6 cells/well) on 12-well Transwell filters (Costar) for 4 days. Efficient knockdown of canine galectin-3 was achieved using the siRNA duplex sequence 5′-AUACCAAGCUGGAUAAUAAUU-3′/

Address for reprint requests and other correspondence: O. Weisz, Renal Electrolyte Div., 978.1 Scaife Hall, 3550 Terrace St., Pittsburgh, PA 15261 (e-mail: weisz@pitt.edu).

3′-GUUAUGGUUCGACCUAUUAUA-5′. Firefly luciferase siRNA was used as a control siRNA (5′-GAAUAUUGUUGCACGAUUUUU-3′/3′-UUCUUAUAACAACGUGCUAAA-5′).

Lipid-based transfection of siRNA duplexes. SiRNA duplexes (1–2 μg) suspended in 500 μl Opti-MEM (GIBCO) were incubated with 5 μl lipofectamine 2000 (Invitrogen) for 30 min at ambient temperature. The transfection mix (125 μl) and 0.5×10^6 MDCK cells in 333 μl of MEM were added to the top chamber of a 12-well Transwell and triturated gently. Experiments were performed 4 days later.

Polarity of biosynthetic delivery assessed using cell surface biotinylation. Domain-selective biotinylation was performed as previously described (20). Briefly, MDCK II cells were grown on filters for 4 days after transfection using the indicated methods. Cells were starved with cysteine-free medium for 30 min, radiolabeled for 2 h with [^{35}S]Cys, then chased in HEPES-buffered MEM for 2 h before apical or basolateral biotinylation. Cells were solubilized and lysates were immunoprecipitated with monoclonal anti-endolyn antibody. After recovery of antibody-antigen complexes, one-fifth of each sample was reserved to calculate the total recovery, and the remainder was incubated with streptavidin to recover biotinylated proteins. Samples were resolved on SDS-PAGE and biotinylation efficiency was quantitated using a phosphorimager (Bio-Rad).

Measurement of polarized secretion. Filter-grown MDCK cells stably expressing GFP-ensol were starved in cysteine-free medium for 30 min, radiolabeled with [^{35}S]Cys for 30 min, and incubated in HEPES-buffered MEM for 90 min at 37°C. The apical and basolateral media were collected separately and the cells were solubilized in detergent-containing solution. Ensol was immunoprecipitated from all samples using monoclonal anti-endolyn antibody. The polarity of ensol secretion was quantitated after SDS-PAGE using a phosphorimager. To assess the secretion of gp80, polarized MDCK cells were incubated in Cys/Met-free medium for 30 min, radiolabeled with [^{35}S]Cys/Met for 2 h, and then incubated in HEPES-buffered MEM for 2 h. Apical and basolateral media were collected from duplicate samples and resolved on SDS-PAGE.

Immunofluorescence microscopy. Mouse antibody 502 against rat endolyn was provided by Dr. G. Ihrke and used at 1:500 dilution. Hybridomas producing anti-p75 and anti-influenza HA antibodies were previously provided by Drs. E. Rodriguez-Boulan and T. Braciale, respectively, and culture supernatants were used at 1:1 dilution. Mouse anti-gp135 was a kind gift of Dr. E. Rodriguez-Boulan and was used at 1:100 dilution. Filter-grown MDCK cells were washed with chilled HEPES-buffered MEM for 15 min and blocked with HEPES-buffered MEM containing BSA for 15 min. To detect surface proteins, cells were incubated with primary antibodies for 1 h on ice, washed extensively, and then incubated with Alexa 488-conjugated goat anti-mouse (Invitrogen; 1:500) for 30 min on ice. Cells were then fixed with 4% paraformaldehyde for 15 min at 37°C and permeabilized with 0.1% (vol/vol) Triton X-100 in PBS-containing glycine and NH_4Cl at ambient temperature for 5 min. Permeabilized cells were incubated sequentially with rat anti-ZO-1 hybridoma tissue culture supernatant (gift of Dr. G. Apodaca; 1:1 dilution) for 30 min at 37°C and Alexa 647-conjugated secondary antibody (Invitrogen, 1:500) for 30 min at ambient temperature. E-cadherin, occludin, and Na^+-K^+-ATPase were detected in fixed and permeabilized cells using mouse anti-E-cadherin antibody (BD Transduction Laboratories), mouse anti-occludin antibody (Invitrogen), and mouse anti-Na^+-K^+-ATPase (abCam), each at 1:100 dilution. To detect cilia, fixed and permeabilized cells were incubated with monoclonal anti-acetylated α-tubulin (Sigma; 1:400) and Alexa 488-conjugated secondary antibody (Invitrogen; 1:500). Confocal images were acquired using a Leica TCS SP microscope equipped with a ×100 HCX PL-APO objective or an Olympus BX61 with a ×100 1.35 NA objective and processed using MetaMorph and Adobe Photoshop software. Cilia length was quantitated from 50 images for each condition using ImageJ software (http://rsb.info.nih.gov/ij/download.html).

Assessment of TJ gate function. TER was determined by applying an EVOM2 epithelial voltohmmeter (WPI). Briefly, control or transfected MDCK cells were cultured on Transwell polycarbonate filters for 4 days. One Transwell chamber was left empty as a control to determine the intrinsic resistance of the filter, which was subtracted from all readings.

To measure paracellular flux, 25 μCi/ml [^{3}H]methoxy-inulin (MP Biomedicals) in 0.5 ml medium were added to the apical chamber of filter-grown MDCK cells (triplicate samples) and the cells were incubated at 37°C. Aliquots (20 μl) of basolateral media were removed at each time point and radioactivity was assessed using a scintillation counter (Wallac).

Integrity of TJ fence function. MDCK cells plated for 4 days after transfection (or not) were mounted in a holder (Bioptechs) on the stage of an Olympus IX81 microscope. FM4–64FX lipophilic styryl dye (100 μM; Invitrogen) was added to the apical chamber of the cells while the basolateral compartment was continuously perfused with PBS supplemented with calcium and magnesium warmed to 37°C. Before image acquisition, the filter membrane was identified and set as the reference plane. During acquisition, images were collected every 5 s at 2.5, 5.0, and 7.5 μm above the reference plane with a ×40 objective (LUCPlanFLN, Olympus). The IX81 was equipped with a xenon lamp (Sutter Instruments) and a wide green filter set (Chroma); exposure time was 300 ms/acquisition. All parameters were controlled using Slidebook 4.2 software (I^3). To quantify the average intensity over time under different transfection conditions, a line was drawn across 10 random cell boundaries per field, and the change in average intensity per minute was determined using MetaMorph. Values were normalized to the average intensity measured in untransfected cells at 0 min.

RESULTS

Nucleofection, but not lipofectamine-mediated transfection, disrupts the polarity of membrane proteins in renal epithelial cells. As a prelude to studies on the mechanism of glycan-dependent apical sorting, we tested approaches to efficiently knock down proteins in polarized MDCK cells using siRNA duplexes. Specifically, we were interested in whether knockdown of galectin-3, a protein reported to be involved in polarized sorting of apical proteins (7), had any effect on the biosynthetic delivery of the sialomucin endolyn. An siRNA duplex targeting canine galectin-3 was designed based on a previously published sequence (7). As a control, we used a commercially available siRNA duplex targeted against luciferase. SiRNA duplexes were introduced into cells by nucleofection or using lipofectamine. After nucleofection, cells were allowed to recover on plastic overnight, trypsinized and counted, and plated onto permeable supports for 4 days. Lipofectamine-treated cells were plated directly onto filters and analyzed 4 days later. As an additional control for both methods, we plated untransfected MDCK cells on filters in parallel with the siRNA-treated samples.

Nucleofection resulted in very high knockdown efficiency of galectin-3 as assessed by Western blotting (Fig. 1*A*). Quantitation of galectin-3 expression using a VersaDoc Imager revealed ~85% reduction in samples nucleofected with galectin-3 siRNA vs. luciferase controls. The efficiency of galectin-3 knockdown mediated by lipofectamine assessed by Western blotting was not as high, but approached 80% (Fig. 1*B*). Both transfection methods yielded similar cDNA transfection efficiencies when tested using a GFP-expressing plasmid (~70% transfection; Suppl. Fig. 1; the online version of this article contains supplemental data).

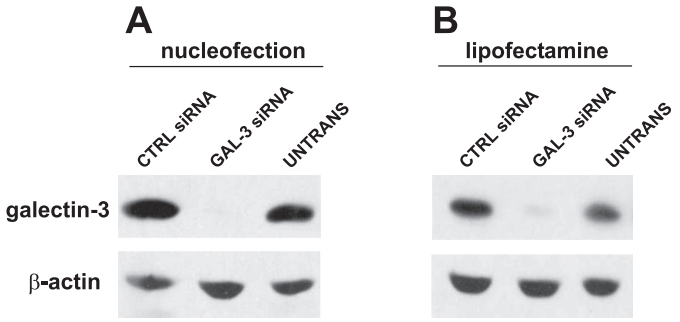

Fig. 1. Introduction of siRNA duplexes by nucleofection and lipofectamine-based transfection results in efficient knockdown of galectin-3 in filter-grown Madin-Darby canine kidney (MDCK) cells. *A*: cells were nucleofected with the indicated siRNAs and plated onto filters the following day. Five days after nucleofection, cells were solubilized and lysates were analyzed by Western blotting to detect galectin-3 or β-actin (as a loading control). Untransfected cells (UNTRANS) plated under identical conditions were included as an additional control. *B*: MDCK cells suspended in MEM were incubated with siRNA duplexes and lipofectamine in the apical chamber of Transwell filter cups. Cells were cultured for 4 days before solubilization and Western blotting. Knockdown efficiency was typically >85% in samples nucleofected with galectin-3 siRNA and slightly lower (~80%) in lipofectamine-treated cells. CTRL, control.

We then assessed the effect of each treatment on polarized delivery of endolyn using a domain-selective biotinylation approach. Three days after being plated, cells were infected with replication-defective recombinant adenovirus-encoding endolyn. In some experiments, stable cell lines expressing endolyn were used, obviating the need for infection. Surprisingly, we routinely observed that endolyn polarity was compromised even in nucleofected cells receiving only control siRNA. In untransfected controls, the polarity of endolyn surface delivery was 73.9% (Fig. 2*A*), consistent with our previous observations (15, 21). In contrast, the apical distribution of endolyn in nucleofected cells was significantly lower (57.6% apical). There was no apparent difference in polarity between cells nucleofected with control vs. galectin-3 siRNA. In contrast, endolyn polarity in lipofectamine-transfected cells was similar to that of untransfected cells (Fig. 2*B*). Moreover, no effect of galectin-3 knockdown on endolyn polarity was observed, suggesting that this lectin is not required for efficient apical delivery of endolyn. Nucleofection also altered the polarized delivery of two other apical markers: the neurotrophin receptor p75 and influenza HA (D. Mo, unpublished results). Whereas endolyn and p75 have glycan-dependent apical targeting information, apical sorting of influenza HA is specified by its transmembrane domain, and this protein takes a distinct route to the apical surface of polarized MDCK cells (6, 15, 17, 29).

We considered the possibility that altered endolyn polarity was due to our specific nucleofection, recovery, or plating conditions. However, varying the number of cells nucleofected or subsequently plated, the cuvette manufacturer, the Amaxa program used (including the T-20 and L-005 programs recommended for epithelial cells including MDCK), and the post-nucleofection recovery conditions did not improve the polarity of endolyn delivery. Substitution of the control (luciferase) siRNA by several other irrelevant siRNA duplexes also disrupted endolyn polarity (D. Mo, unpublished results).

Our biochemical experiments suggested that polarized delivery of membrane proteins might be compromised in nucleofected cells. To test whether steady-state distribution of membrane proteins was altered, we used indirect immunofluorescence to examine surface endolyn distribution in nucleofected vs. untransfected MDCK cells. As shown in Fig. 3*A*, surface endolyn was localized primarily to the apical membrane of untransfected controls. In contrast, endolyn was also clearly visible at the basolateral surface of cells nucleofected with either control or galectin-3 siRNA. Similar results were also observed in MDCK cells expressing p75 and HA. However, the distributions of the endogenous apical protein gp135 and the laterally localized proteins E-cadherin and Na^+-K^+-ATPase were not affected by nucleofection. To confirm that the relocalization is not cell-type specific, endolyn polarity was also examined in nucleofected, lipofectamine-treated, and control (untransfected) mouse CCD cells. As in MDCK cells, endolyn was less apically polarized in nucleofected cells compared with lipofectamine-treated or untransfected cells (Fig.

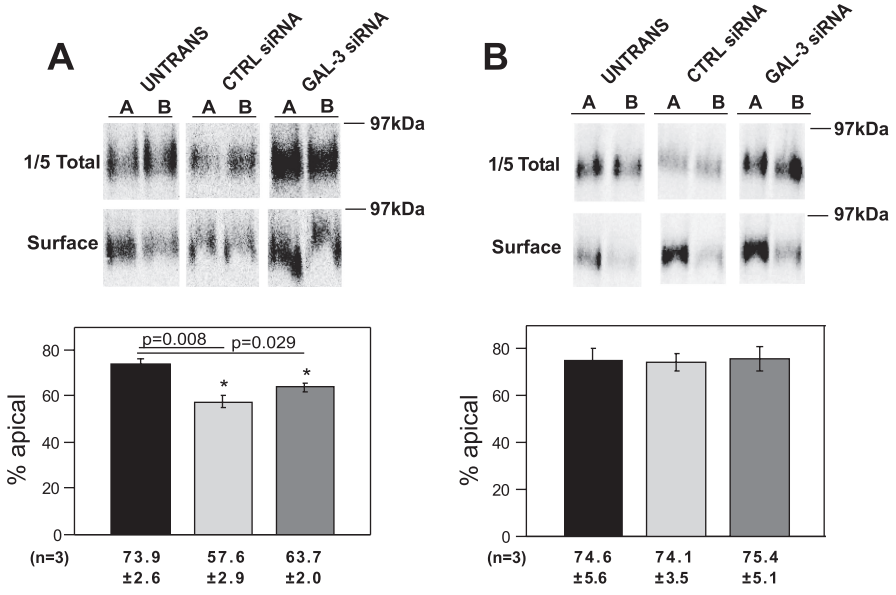

Fig. 2. Nucleofection, but not lipofectamine, compromises the apical delivery of the transmembrane sialomucin endolyn. *A*: nucleofected or control untransfected endolyn-expressing MDCK cells were starved in cys-free medium for 30 min, radiolabeled with [^{35}S]cys for 2 h, and chased for 2 h. The apical or basolateral surface of duplicate filters was biotinylated and the polarity of endolyn delivery was quantitated as described in MATERIALS AND METHODS. A representative gel showing total and surface endolyn recovered from apically (A) and basolaterally (B) biotinylated samples is shown. Endolyn polarity in 3 independent experiments (means ± SE) each performed in duplicate or triplicate is plotted. *$P < 0.05$ vs. untransfected cells by ANOVA. *B*: polarity of endolyn cell surface delivery was assessed as described above in filter-grown untransfected or lipofectamine-treated MDCK cells. A representative gel is shown and the results of 3 experiments, each performed in duplicate or triplicate, are plotted (means ± SE).

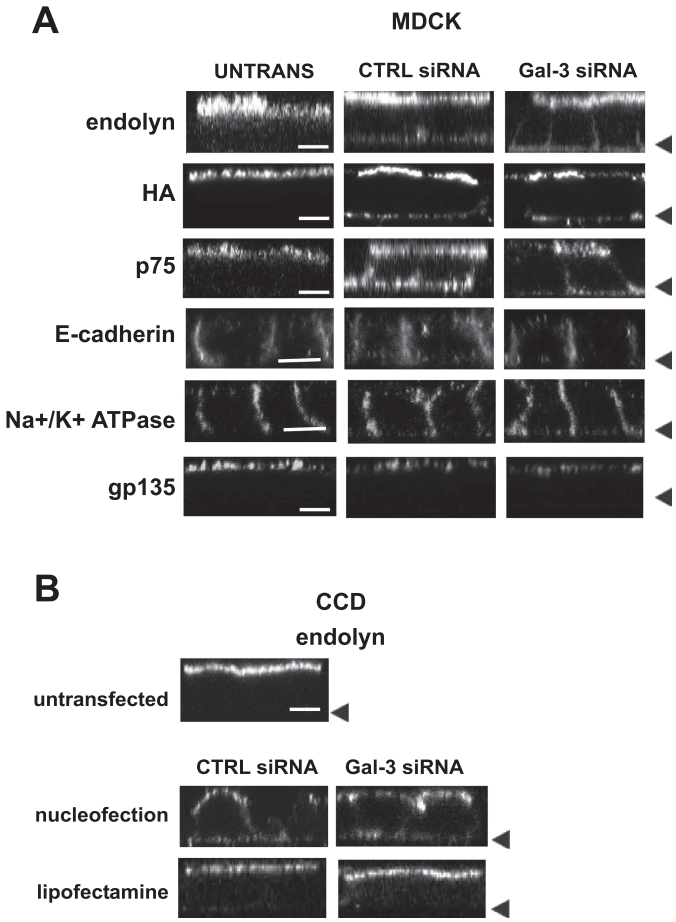

Fig. 3. Nucleofection alters the steady-state distribution of transmembrane proteins. *A*: control (untransfected) or nucleofected MDCK cells plated on 12-well filters for 4 days were incubated on ice with primary antibodies against endolyn, p75, hemagglutinin (HA), or gp135 and Alexa 488-conjugated secondary antibodies before fixation. E-cadherin and Na^+-K^+-ATPase were detected in cells permeabilized after fixation. Cells were visualized by confocal microscopy and representative XZ sections are shown. Arrowheads mark the position of the filter in each row. *B*: similar experiments were performed to visualize endolyn distribution in control, nucleofected, and lipofectamine-transfected mouse cortical collecting duct (CCD) cells. Bar = 10 μm.

3*B*). Additionally, to determine whether the altered localization is transient, endolyn distribution was assessed at 4, 6, 8, and 10 days postnucleofection and found to be compromised at each time point (Suppl. Fig. 2).

We next tested whether nucleofection alters the targeting of secreted proteins in polarized cells. To address this, we examined the release of a truncated form of endolyn called ensol. We previously showed that apical secretion of ensol was very efficient (~85%) (20). Interestingly, nucleofection had no effect on the fidelity of ensol secretion (Fig. 4). The polarity of secretion of the endogenous protein complex gp80 was also not affected by nucleofection (D. Mo, unpublished results). This suggests that nucleofection selectively alters the polarized distribution of transmembrane but not secreted proteins, and therefore might reflect a postdelivery event rather than a change in biosynthetic sorting efficiency.

Cilia morphology is unaffected by nucleofection. Primary cilia play an increasingly appreciated role in the development of cell polarity, and defects in ciliary length or formation have been implicated in renal disease (5, 16, 19, 27). We therefore tested whether nucleofection alters ciliary length in polarized MDCK cells. Cilia in untransfected, nucleofected, or lipofectamine-treated cells were visualized using anti-tubulin antibodies, and their length was assessed using ImageJ software. There was no qualitative difference in the number of cilia observed per field under these different conditions (Fig. 5*A*). Moreover, we found no variation in ciliary length in nucleofected cells compared with untransfected or lipofectamine-treated cells (Fig. 5*B*).

Fence functions of TJs are disrupted in nucleofected cells. Another possibility to explain the alteration in membrane polarity of nucleofected cells is a defect in TJ formation or function. Nucleofected cells had similar ZO-1 and occludin-staining patterns compared with untransfected controls (Fig. 6), suggesting that the morphology of TJs is not grossly aberrant. We next examined TJ function using several approaches. To assess the gate function of TJs, we monitored the diffusion of the small molecule tracer [^{3}H]inulin. As shown in Fig. 7*A*, inulin permeability across untransfected, lipofectamine-treated, and nucleofected monolayers was comparable, suggesting that the integrity of the gate function was intact under all conditions. Additionally, we found no significant difference in the TER across filter-grown monolayers (untransfected cells: 101.4 ± 17.4 Ω·cm^2; nucleofected cells: 94.4 ± 6.0 Ω·cm^2; lipofectamine-treated cells: 112.8 ± 9.5 Ω·cm^2).

We next examined the diffusion barrier or "fence" function of TJs by testing whether compartmentalization of the lipophilic styryl dye FM4–64FX was compromised in nucleofected cells. Previous studies used this approach to test for defects in TJ fence function (22, 28). FM4–64FX was added to the apical chamber of untransfected, nucleofected, or lipofectamine-treated MDCK cells grown on filters for 4 days, and image stacks were acquired every 5 s for 5 min after addition of the dye. Figure 7 shows the time-dependent accumulation of FM4–64FX fluorescence at the lateral membrane of cells in an optical slice centered at 2.5 μm above the filter for each

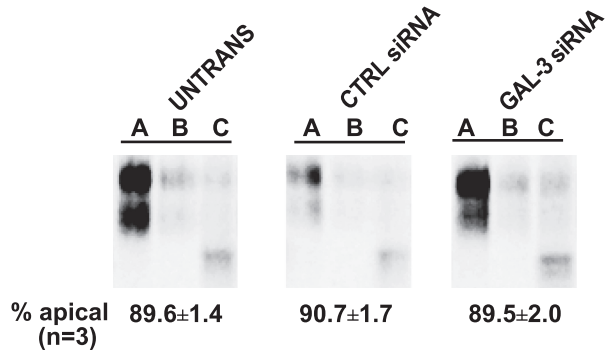

Fig. 4. Polarized secretion of a soluble protein is not affected by nucleofection. Filter-grown MDCK cells were subjected to Amaxa nucleofection with the indicated siRNA duplexes. The following day, nucleofected and control untransfected cells were plated on filters and protein secretion of a truncated mutant of endolyn (ensol) tagged with GFP was analyzed 4 days later. Cells were radiolabeled with [^{35}S]cys for 30 min and chased for 1.5 h. The apical and basolateral media were collected separately, and the cells were solubilized. Samples were immunoprecipitated using anti-endolyn antibody and analyzed by SDS-PAGE. Representative samples from one experiment are shown and the quantitation of apically secreted ensol in 3 independent experiments performed in triplicate is noted below each condition. A, apical; B, basolateral; C, cell.

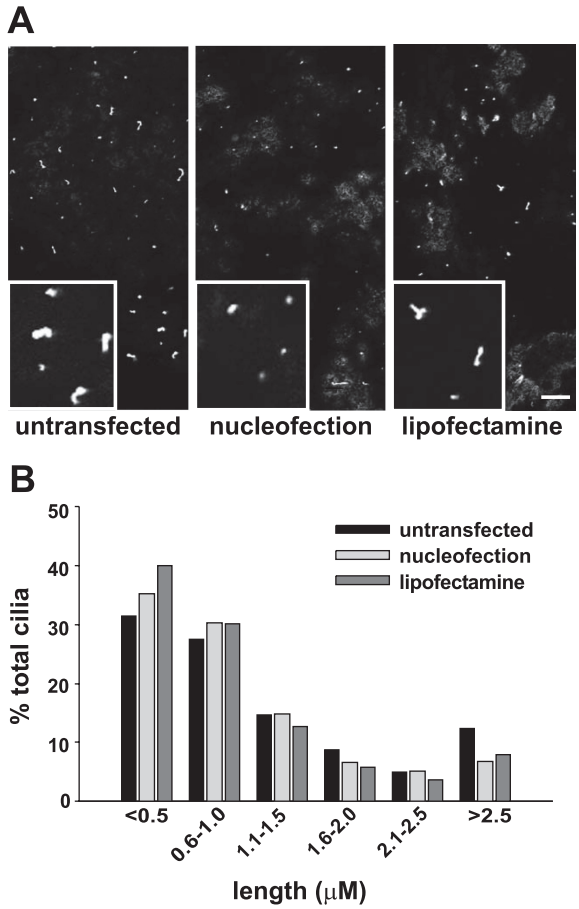

Fig. 5. Nucleofection does not alter cilia length. MDCK cells treated as indicated were plated on filters for 4 days and then fixed and processed for indirect immunofluorescence using monoclonal anti-acetylated β-tubulin antibody. *A*: representative confocal image and *inset* for each condition. Bar = 10 μm. *B*: ImageJ software was used to measure the distribution of cilia lengths from 50 randomly acquired images for each condition.

condition. Strikingly, whereas little to no diffusion of apically added FM4–64FX to the lateral surface was observed in untransfected and lipofectamine-transfected cells, we observed rapid diffusion of the dye in nucleofected cells (Fig. 7*B*). Quantitation of two independent experiments confirmed an approximately twofold increase in the rate of FM4–64FX diffusion in nucleofected cells vs. untransfected or lipofectamine-treated cells (Fig. 7*C*). This result indicates that the diffusion barrier between apical and basolateral membranes is disrupted in nucleofected cells and is consistent with the selective disruption in membrane but not secreted protein polarity that we observed in these cells.

DISCUSSION

Here, we compared the effects of nucleofection vs. lipofectamine-based transfection methods on the development of polarity in MDCK cells. We found that the distribution of several transmembrane cell surface proteins was disrupted in MDCK and CCD cells that had been nucleofected with control (irrelevant) siRNA duplexes. However, apical sorting of secreted proteins was unaffected by this treatment. Varying numerous facets of the experimental protocol did not rescue the defects in polarity. In contrast, cells transfected using lipofectamine exhibited normal membrane protein polarity, comparable to untransfected cells. Studies to independently test the fence and gate functions of TJs revealed a selective defect in the membrane diffusion barrier in nucleofected cells, whereas transepithelial passage of ions and small molecule tracers was unaffected. Our results suggest that renal epithelial cells subjected to nucleofection are unable to develop fully functional TJs even after 5–9 days on filters. These studies have important implications for the design and interpretation of siRNA knockdown experiments in polarized cell lines.

Our studies suggest that biosynthetic sorting of newly synthesized proteins may be unaffected in nucleofected cells and that polarity is lost after surface delivery as a result of compromised TJ fence function. Interestingly, we did not detect any striking changes in the steady-state distribution of three endogenous proteins (gp135, E-cadherin, and Na^+-K^+-ATPase) after nucleofection. The differences we observed between endogenous vs. heterologously expressed proteins might reflect differential assay sensitivity due to the lower abundance of endogenous proteins. Alternatively, endogenous proteins may be better retained at the appropriate plasma membrane domain as a result of their normal interactions with cytoskeletal or other surface-resident proteins.

TJs are a complex assembly of transmembrane and cytoplasmic proteins that play a role in both the establishment and the maintenance of epithelial cell polarity (reviewed in Refs. 3, 24). The gate function prevents paracellular diffusion of water, ions, and metabolites by regulating movement between adjacent epithelial cells. The fence function prevents the diffusion of transmembrane proteins and outer leaflet lipids. Our results suggest that nucleofection selectively compromises TJ fence but not gate function.

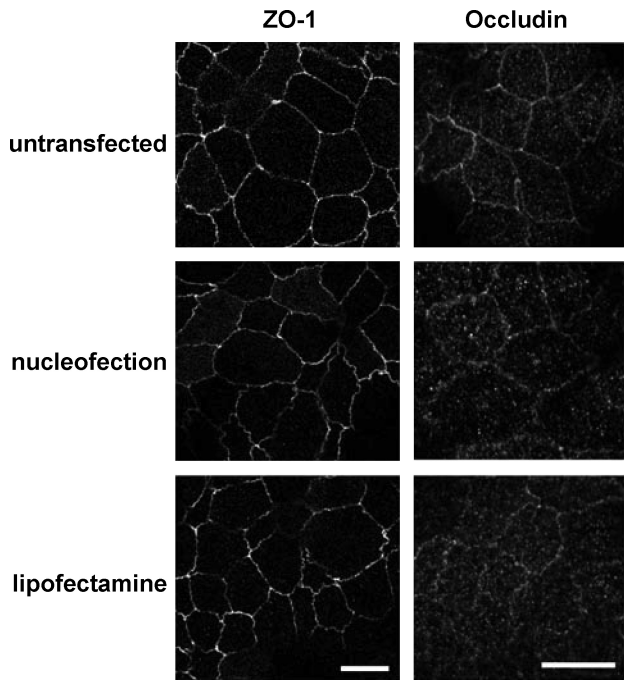

Fig. 6. Localization of tight junction markers is not affected in nucleofected cells. Untransfected, nucleofected, and lipofectamine-transfected cells were fixed and processed for indirect immunofluorescence to detect the tight junction markers ZO-1 and occludin. Scale bar = 10 μm.

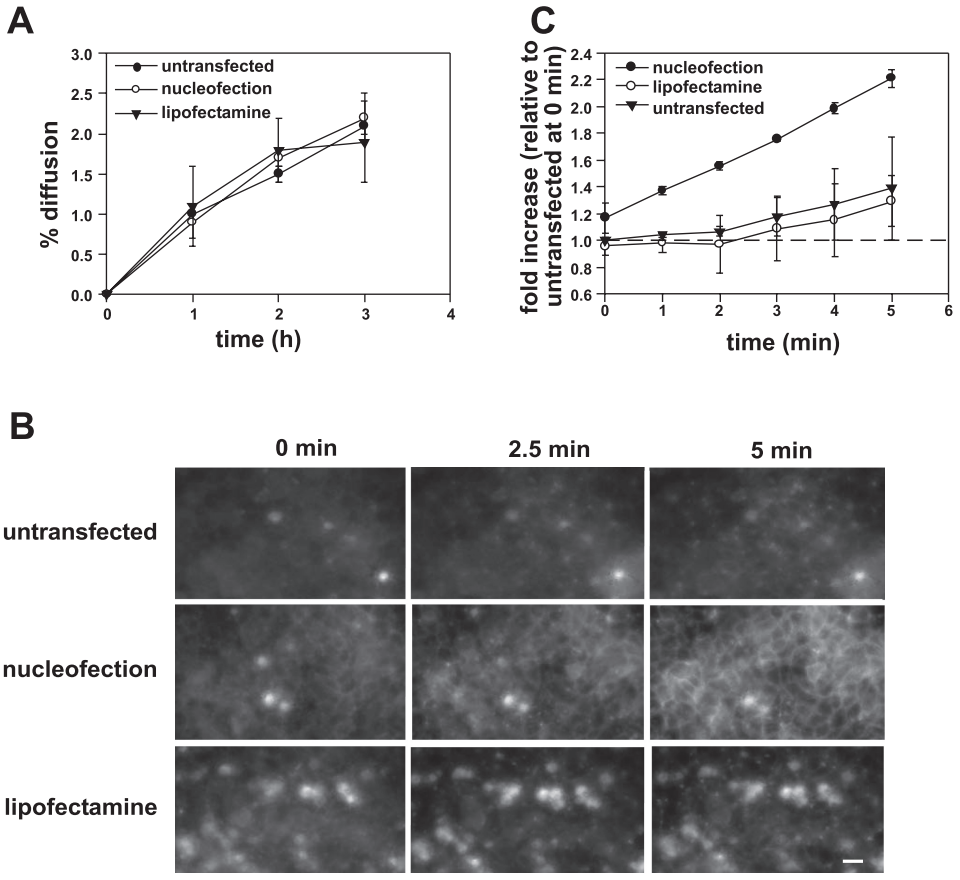

Fig. 7. Tight junction fence, but not gate function, is disrupted in nucleofected cells. *A*: kinetics of transepithelial [^{3}H]inulin diffusion across filter-grown MDCK cells. *B*: FM4–64FX (100 μM) was added to the apical chamber of filter-grown MDCK cells that had been previously treated as indicated. Cells were imaged every 5 s for 5 min and optical slices collected 2.5 μm above the level of the filters at 0, 2.5, and 5 min after addition of the dye are shown. All images were acquired and processed using identical conditions. The bright spots represent out-of-focus fluorescence from apoptotic cells above the cell monolayer and were especially prominent in lipofectamine-treated samples. Bar = 10 μm. *C*: change in intensity of FM4–64FX staining at the lateral surface over time was quantified in 2 independent experiments and is plotted relative to the initial intensity measured at *time 0* in untransfected cells.

While numerous TJ components have been identified, how gate and fence function are modulated is largely unknown. Inhibiting the function of TJ transmembrane proteins such as occludin, claudins, and junctional adhesion molecules, using antibodies or by overexpression expression or knockdown, generally disrupts the permeability barrier (gate) of polarized epithelial cells without apparently affecting membrane or lipid diffusion across the TJ boundary (1, 8, 18, 25, 26, 30).

A few studies described maneuvers that disrupt both TJ gate and fence functions. For example, expression of a mutant of occludin lacking its COOH terminus increased paracellular flux as well as lipid diffusion across the TJ of MDCK cells, although the polarity of membrane proteins was unaffected (1). Similarly, siRNA-mediated knockdown of ZO-2 disrupted both gate and fence functions of TJs (14). However, only one other report that we are aware of observed a selective defect in TJ fence function with no change in TER. In that study, addition of an antibody directed against the second extracellular loop of occludin resulted in both altered membrane polarity and lipid diffusion in T84 cells (25).

Our results do not address why nucleofection disrupts the establishment of a polarized phenotype. Nucleofection physically creates transient pores in the plasma membrane and nucleus using high-intensity electrical pulses to facilitate the entry of foreign molecules (23). The pores begin to reseal after the removal of the external field. It is possible that the incubation solutions and/or the electrical pulse itself initiate signal transduction cascades that have long-term consequences on gene expression. Interestingly, whereas most aspects of cell function that we tested are unaffected by this procedure, there appears to be a selective defect in the maintenance of the membrane diffusion barrier. Several possibilities might account for this, including alterations in plasma membrane lipid composition or in the expression of proteins involved in maintaining cell polarity. Regardless of the mechanism, our results suggest that nucleofection of even irrelevant siRNA duplexes compromises the subsequent development of renal epithelial cell polarity, limiting its utility for studies using these cells. In contrast, transfection of siRNA duplexes using lipid-based approaches provides comparable knockdown efficiency without disruption of cell polarity.

ACKNOWLEDGMENTS

We are grateful to Drs. G. Ihrke, G. Apodaca, T. Braciale, and E. Rodriguez-Boulan for generous gifts of antibodies and hybridoma lines, and to Dr. P. Mattila for help with image acquisition.

GRANTS

This work was supported by National Institutes of Health Grant DK-054407 (to O. A. Weisz) and by the Assay Core of the CF Research Center (CFF Grant R883-CR02). We thank the morphology and physiology cores of the Pittsburgh Center for Kidney Research (P30-DK-079307) for technical assistance.

DISCLOSURES

No conflicts of interest, financial or otherwise, are declared by the author(s).

Present address of B. A. Potter: Dept. of Biology, The Behrend College, Pennsylvania State Univ., Erie, PA 16563.

REFERENCES

1. **Balda MS, Whitney JA, Flores C, Gonzalez S, Cereijido M, Matter K.** Functional dissociation of paracellular permeability and transepithelial electrical resistance and disruption of the apical-basolateral intramembrane diffusion barrier by expression of a mutant tight junction membrane protein. *J Cell Biol* 134: 1031–1049, 1996.
2. **Bens M, Vallet V, Cluzeaud F, Pascual-Letallec L, Kahn A, Rafestin-Oblin ME, Rossier BC, Vandewalle A.** Corticosteroid-dependent sodium transport in a novel immortalized mouse collecting duct principal cell line. *J Am Soc Nephrol* 10: 923–934, 1999.
3. **Cereijido M, Contreras RG, Shoshani L, Flores-Benitez D, Larre I.** Tight junction and polarity interaction in the transporting epithelial phenotype. *Biochim Biophys Acta* 1778: 770–793, 2008.
4. **Chen X, Macara IG.** RNA interference techniques to study epithelial cell adhesion and polarity. *Methods Enzymol* 406: 362–374, 2006.
5. **Chiu MG, Johnson TM, Woolf AS, Dahm-Vicker EM, Long DA, Guay-Woodford L, Hillman KA, Bawumia S, Venner K, Hughes RC, Poirier F, Winyard PJ.** Galectin-3 associates with the primary cilium and modulates cyst growth in congenital polycystic kidney disease. *Am J Pathol* 169: 1925–1938, 2006.
6. **Cresawn KO, Potter BA, Oztan A, Guerriero CJ, Ihrke G, Goldenring JR, Apodaca G, Weisz OA.** Differential involvement of endocytic compartments in the biosynthetic traffic of apical proteins. *EMBO J* 26: 3737–3748, 2007.
7. **Delacour D, Cramm-Behrens CI, Drobecq H, Le Bivic A, Naim HY, Jacob R.** Requirement for galectin-3 in apical protein sorting. *Curr Biol* 16: 408–414, 2006.
8. **Furuse M, Hata M, Furuse K, Yoshida Y, Haratake A, Sugitani Y, Noda T, Kubo A, Tsukita S.** Claudin-based tight junctions are crucial for the mammalian epidermal barrier: a lesson from claudin-1-deficient mice. *J Cell Biol* 156: 1099–1111, 2002.
9. **Gresch O, Engel FB, Nesic D, Tran TT, England HM, Hickman ES, Korner I, Gan L, Chen S, Castro-Obregon S, Hammermann R, Wolf J, Muller-Hartmann H, Nix M, Siebenkotten G, Kraus G, Lun K.** New nonviral method for gene transfer into primary cells. *Methods* 33: 151–163, 2004.
10. **Hamm A, Krott N, Breibach I, Blindt R, Bosserhoff AK.** Efficient transfection method for primary cells. *Tissue Eng* 8: 235–245, 2002.
11. **Hardy S, Kitamura M, Harris-Stansil T, Dai Y, Phipps ML.** Construction of adenovirus vectors through Cre-lox recombination. *J Virol* 71: 1842–1849, 1997.
12. **Henkel JR, Apodaca G, Altschuler Y, Hardy S, Weisz OA.** Selective perturbation of apical membrane traffic by expression of influenza M2, an acid-activated ion channel, in polarized Madin-Darby canine kidney cells. *Mol Biol Cell* 9: 2477–2490, 1998.
13. **Henkel JR, Weisz OA.** Influenza virus M2 protein slows traffic along the secretory pathway. pH perturbation of acidified compartments affects early Golgi transport steps. *J Biol Chem* 273: 6518–6524, 1998.
14. **Hernandez S, Chavez Munguia B, Gonzalez-Mariscal L.** ZO-2 silencing in epithelial cells perturbs the gate and fence function of tight junctions and leads to an atypical monolayer architecture. *Exp Cell Res* 313: 1533–1547, 2007.
15. **Ihrke G, Bruns JR, Luzio JP, Weisz OA.** Competing sorting signals guide endolyn along a novel route to lysosomes in MDCK cells. *EMBO J* 20: 6256–6264, 2001.
16. **Koch A, Poirier F, Jacob R, Delacour D.** Galectin-3, a novel centrosome-associated protein, required for epithelial morphogenesis. *Mol Biol Cell* 21: 219–231, 2010.
17. **Lin S, Naim HY, Rodriguez AC, Roth MG.** Mutations in the middle of the transmembrane domain reverse the polarity of transport of the influenza virus hemagglutinin in MDCK epithelial cells. *J Cell Biol* 142: 51–57, 1998.
18. **Liu Y, Nusrat A, Schnell FJ, Reaves TA, Walsh S, Pochet M, Parkos CA.** Human junction adhesion molecule regulates tight junction resealing in epithelia. *J Cell Sci* 113: 2363–2374, 2000.
19. **Overgaard CE, Sanzone KM, Spiczka KS, Sheff DR, Sandra A, Yeaman C.** Deciliation is associated with dramatic remodeling of epithelial cell junctions and surface domains. *Mol Biol Cell* 20: 102–113, 2009.
20. **Potter BA, Ihrke G, Bruns JR, Weixel KM, Weisz OA.** Specific N-glycans direct apical delivery of transmembrane, but not soluble or glycosylphosphatidylinositol-anchored forms of endolyn in Madin-Darby canine kidney cells. *Mol Biol Cell* 15: 1407–1416, 2004.
21. **Potter BA, Weixel KM, Bruns JR, Ihrke G, Weisz OA.** N-glycans mediate apical recycling of the sialomucin endolyn in polarized MDCK cells. *Traffic* 7: 146–154, 2006.
22. **Rojas R, Ruiz WG, Leung SM, Jou TS, Apodaca G.** Cdc42-dependent modulation of tight junctions and membrane protein traffic in polarized Madin-Darby canine kidney cells. *Mol Biol Cell* 12: 2257–2274, 2001.
23. **Rols MP.** Mechanism by which electroporation mediates DNA migration and entry into cells and targeted tissues. *Methods Mol Biol* 423: 19–33, 2008.
24. **Shin K, Fogg VC, Margolis B.** Tight junctions and cell polarity. *Annu Rev Cell Dev Biol* 22: 207–235, 2006.
25. **Tokunaga Y, Kojima T, Osanai M, Murata M, Chiba H, Tobioka H, Sawada N.** A novel monoclonal antibody against the second extracellular loop of occludin disrupts epithelial cell polarity. *J Histochem Cytochem* 55: 735–744, 2007.
26. **Van Itallie CM, Anderson JM.** Claudins and epithelial paracellular transport. *Annu Rev Physiol* 68: 403–429, 2006.
27. **Verghese E, Ricardo SD, Weidenfeld R, Zhuang J, Hill PA, Langham RG, Deane JA.** Renal primary cilia lengthen after acute tubular necrosis. *J Am Soc Nephrol* 20: 2147–2153, 2009.
28. **Wakabayashi Y, Chua J, Larkin JM, Lippincott-Schwartz J, Arias IM.** Four-dimensional imaging of filter-grown polarized epithelial cells. *Histochem Cell Biol* 127: 463–472, 2007.
29. **Yeaman C, Le Gall AH, Baldwin AN, Monlauzeur L, Le Bivic A, Rodriguez-Boulan E.** The O-glycosylated stalk domain is required for apical sorting of neurotrophin receptors in polarized MDCK cells. *J Cell Biol* 139: 929–940, 1997.
30. **Yu AS, McCarthy KM, Francis SA, McCormack JM, Lai J, Rogers RA, Lynch RD, Schneeberger EE.** Knockdown of occludin expression leads to diverse phenotypic alterations in epithelial cells. *Am J Physiol Cell Physiol* 288: C1231–C1241, 2005.